NANO LETTERS

2008
Vol. 8, No. 4
1197-1201

Spin-Polarizable Excitonic Luminescence in Colloidal Mn^{2+}-Doped CdSe Quantum Dots

Rémi Beaulac,[†] Paul I. Archer,[†] Xinyu Liu,[‡] Sanghoon Lee,[§] G. Mackay Salley,[†] Margaret Dobrowolska,[‡] Jacek K. Furdyna,[‡] and Daniel R. Gamelin*[,†]

Department of Chemistry, University of Washington, Seattle, Washington 98195, Department of Physics, University of Notre Dame, Notre Dame, Indiana 46556, and Department of Physics, Korea University, Seoul 136-701, Republic of Korea

Received January 21, 2008; Revised Manuscript Received February 19, 2008

ABSTRACT

The photoluminescence of colloidal Mn^{2+}-doped CdSe nanocrystals has been studied as a function of nanocrystal diameter. These nanocrystals are shown to be unique among colloidal doped semiconductor nanocrystals reported to date in that quantum confinement allows tuning of the CdSe bandgap energy across the Mn^{2+} excited-state energies. At small diameters, the nanocrystal photoluminescence is dominated by Mn^{2+} emission. At large diameters, CdSe excitonic photoluminescence dominates. The latter scenario has allowed spin-polarized excitonic photoluminescence to be observed in colloidal doped semiconductor nanocrystals for the first time.

Colloidal transition-metal-doped semiconductor nanocrystals[1] are attracting broad interest in fields as diverse as spintronics,[2–7] phosphor technologies,[3,8–10] bioimaging,[11,12] and fundamental synthetic and physical inorganic chemistries.[4,13–15] Although doping with transition-metal ions can impart remarkable magneto-optical properties to quantum dots, an undesirable side effect is that it also often leads to quenching of excitons by energy transfer to the dopants.[3,8–10,16] Here we report the first demonstration of colloidal doped semiconductor nanocrystals in which excitonic emission is retained upon doping and coexists with strong dopant−exciton magnetic exchange coupling. This scenario is achieved in Mn^{2+}-doped CdSe (Mn^{2+}:CdSe) nanocrystals by using quantum confinement to tune the excitonic levels to below all Mn^{2+} excited states. These colloidal nanocrystals show magneto-optical properties comparable to those of analogous quantum dots grown by molecular beam epitaxy (MBE) and therefore introduce new opportunities for assembly of nanoscale spin-based information processing devices by soft chemical techniques.

Colloidal quantum dots (QDs) doped with Mn^{2+} can be organized into three general groups according to their electronic structures, which define their photophysical and magneto-optical properties. In most cases, the Mn^{2+} ligand-field states reside within the optical gap of the host semiconductor (scenario I in Figure 1). Colloidal doped nanocrystals of this type are of particular interest for photo- or electro-luminescence applications because semiconductor excitation leads to rapid energy transfer to the Mn^{2+} dopants ($k_{ET}^{Mn^{2+}} \gg 0$), which can themselves emit with high quantum yields. Examples include colloidal Mn^{2+}-doped ZnS, ZnSe, and CdS QDs.[2,3,8,10,12] A rarer situation occurs in wide-gap semiconductors, where donor- or acceptor-type photoionization states within the gap can introduce nonradiative relaxation pathways that largely or entirely quench the nanocrystal emission (scenario II in Figure 1). A thoroughly studied example is the case of colloidal Mn^{2+}-doped ZnO nanocrystals, which possess a sub-bandgap donor-type photoionization level.[7] A third distinct scenario can be identified when no impurity states exist within the gap of the host semiconductor (scenario III in Figure 1). In many regards, this third scenario is the most interesting and fundamentally important because the size-tunable emission, lasing capabilities, and other attractive photophysical properties of colloidal undoped semiconductor QDs can be retained, while the Mn^{2+} impurities introduce an additional degree of freedom for controlling those physical properties. Although many syntheses have been attempted, to date there has been no experimental demonstration of any signature diluted magnetic semiconductor (DMS) characteristic for any colloidal doped semiconductor nanocrystals representative of scenario III in Figure 1 (see Supporting Information).

To explore scenario III, colloidal Mn^{2+}-doped CdSe nanocrystals of different sizes were prepared (see Supporting Information). Figure 2 shows absorption and luminescence

* Corresponding author. E-mail: Gamelin@chem.washington.edu.
† Department of Chemistry, University of Washington.
‡ Department of Physics, University of Notre Dame.
§ Department of Physics, Korea University.

10.1021/nl080195p CCC: $40.75
Published on Web 03/11/2008

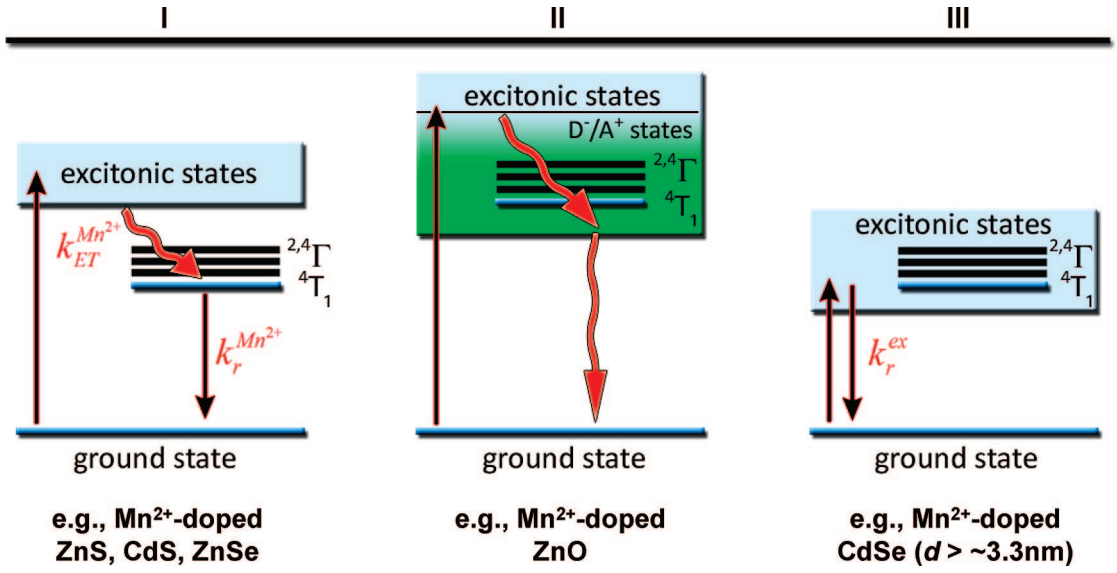

Figure 1. Schematic representation of different electronic structures related to photoluminescence observed in colloidal Mn^{2+}-doped semiconductor nanocrystals. In the first scenario (I), efficient energy transfer ($k_{ET}^{Mn^{2+}}$) quenches excitonic emission and sensitizes Mn^{2+} $^6A_1 \leftarrow {}^4T_1$ luminescence. In the second scenario (II), excitons are quenched by Mn^{2+} photoionization states (dopant-bound excitons) that relax nonradiatively to the ground state. In the third scenario (III), all Mn^{2+} excited states are located outside of the bandgap, and the nanocrystals show excitonic emission. Examples of Mn^{2+}-doped II−VI DMS nanocrystals of each type are provided.

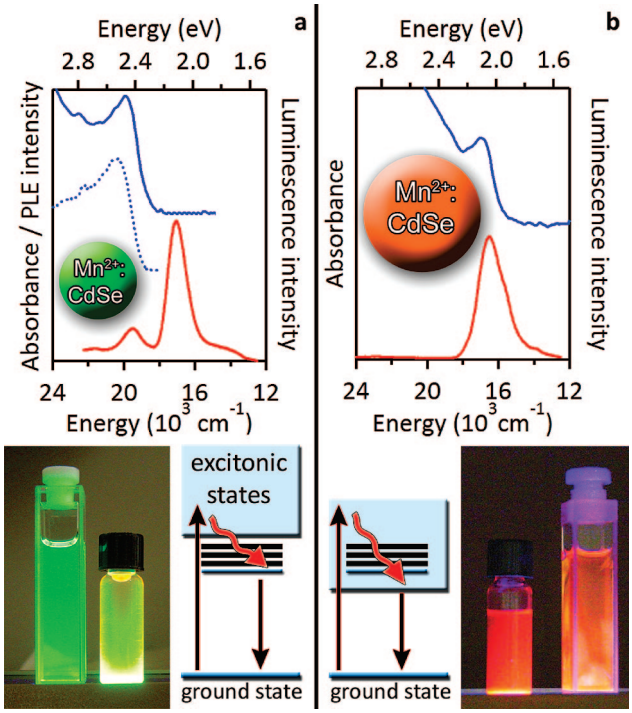

Figure 2. Change of the nature of the emissive state with size in colloidal Mn^{2+}:CdSe quantum dots. 5 K absorption and photoluminescence spectra of (a), small ($d \approx 2.6$ nm 0.9% Mn^{2+}) and (b), large ($d \approx 4.0$ nm 1.4% Mn^{2+}) colloidal Mn^{2+}:CdSe quantum dots. Mn^{2+} $^6A_1 \leftarrow {}^4T_1$ emission dominates in the sample of small nanocrystals (scenario I in Figure 1), whereas only excitonic emission is observed in the larger nanocrystals (scenario III in Figure 1). In (a), the photoluminescence excitation profile for the Mn^{2+} emission is shown as a dotted line. The photos show the emitting nanocrystal colloidal suspensions.

spectra of $d \approx 2.6$ and 4.0 nm colloidal Mn^{2+}:CdSe QDs, along with photographs of the emitting colloids. For the smaller of the two (Figure 2a), two luminescence peaks are observed. The higher-energy peak coincides with the first exciton of the CdSe nanocrystals observed in the absorption spectrum. The lower-energy luminescence peak is readily attributable to the $^6A_1 \leftarrow {}^4T_1$ ligand-field transition of Mn^{2+}, analogous to previously synthesized Mn^{2+}-doped nanocrystals.[2,3,8,10,12] This $^6A_1 \leftarrow {}^4T_1$ photoluminescence intensity decays with a long lifetime of several hundred microseconds at 10 K. A detailed report on the photoluminescence lifetimes of these samples will be presented elsewhere. Photoluminescence excitation (PLE) spectra collected by monitoring the Mn^{2+} $^6A_1 \leftarrow {}^4T_1$ transition mimic the absorption spectrum (Figure 2a), demonstrating that the Mn^{2+} emission is sensitized by CdSe QD excitation (i.e., $k_{ET}^{Mn^{2+}} \gg 0$) and hence that the exciton is quenched by Mn^{2+} doping. The excitonic emission that remains is most likely due to the presence of some undoped nanocrystals, the likelihood of which increases as the particle dimensions decrease.[5,13] These nanocrystals are thus described by scenario I of Figure 1. Interestingly, Mn^{2+} luminescence in colloidal Mn^{2+}:CdSe QDs has not been reported previously, despite several prior claims regarding synthesis of this material.[13,17–20] Even in reports of Mn^{2+}:CdSe QDs prepared by MBE, the Mn^{2+} luminescence is often weak or absent.[16,21–23] The data in Figure 2a thus provide the first clear evidence that sensitized Mn^{2+} emission dominates the luminescence of small Mn^{2+}:CdSe nanocrystals. In contrast, the photoluminescence spectrum of the larger nanocrystals shows only one major feature, which coincides with the first absorption maximum and is therefore attributed to excitonic emission. The Mn^{2+} emission would occur at higher energy but is not clearly observed.

Figure 3a presents photoluminescence spectra of a series of colloidal Mn^{2+}:CdSe QDs with 2 nm $< d <$ 5 nm, and Figure 3b plots the energies of the Mn^{2+} and excitonic

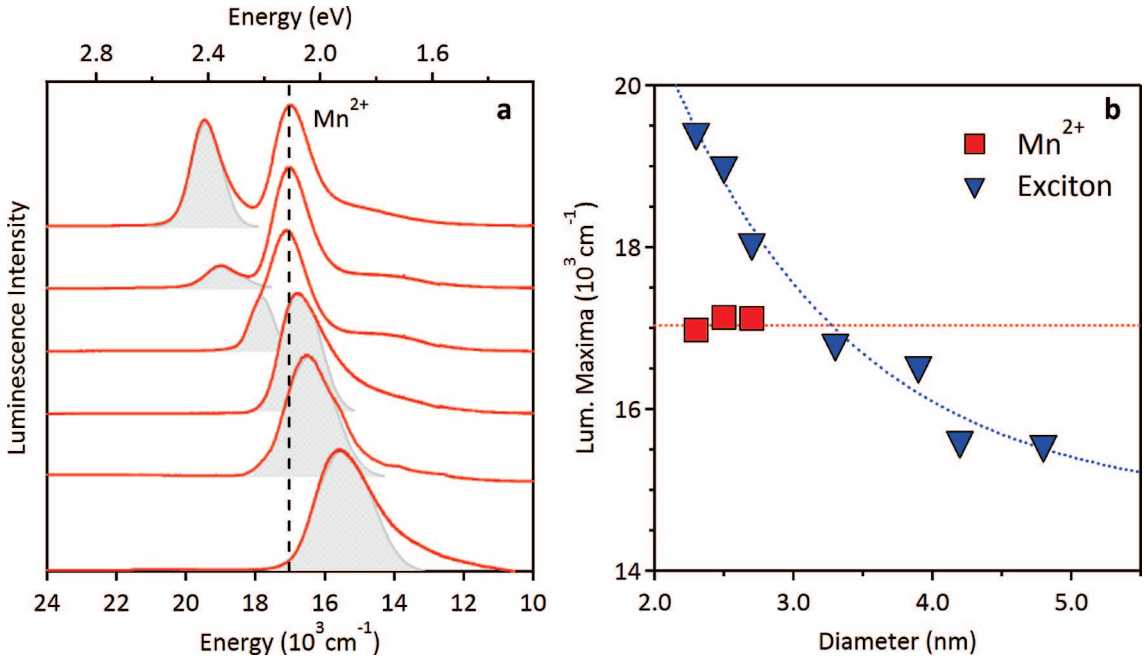

Figure 3. Mn^{2+}:CdSe quantum dot photoluminescence as a function of nanocrystal diameter. (a) Low-temperature (5 K) photoluminescence spectra of a series of Mn^{2+}:CdSe quantum dots with $d = 2.3$, 2.5, 2.7, 3.3, 3.9, and 4.2 nm (top to bottom). The vertical broken line shows the energy of the Mn^{2+} $^6A_1 \leftarrow {}^4T_1$ luminescence (maximum: 17200 cm^{-1}, or 2.11 eV), observed only in the smallest samples. (b) Energies of the Mn^{2+} $^4T_1$ and CdSe excitonic photoluminescence maxima plotted vs Mn^{2+}:CdSe nanocrystal diameter. The two cross at $d \approx 3.3$ nm.

photoluminescence peaks from Figure 3a as a function of nanocrystal diameter. Whereas the energy of the excitonic transition depends strongly on particle size, the energy of the Mn^{2+} transition does not. Interpolation indicates that the nature of the emissive state changes at around $d \approx 3.3$ nm. This point marks the transition between scenarios I and III in Figure 1. The largest Mn^{2+}:CdSe nanocrystals thus show unquenched excitonic emission despite the presence of Mn^{2+} dopants.

The defining feature of a DMS is the "giant" Zeeman splitting, which arises from magnetic exchange interactions between delocalized charge carriers and the magnetic dopants[24] and which is responsible for all of the physical properties of this class of materials relevant to spintronics. Magneto-optical spectroscopies can be used to probe such Zeeman splittings directly. Magnetic circular dichroism (MCD) spectroscopy has been applied previously to study the excitonic Zeeman splittings of various colloidal semiconductor nanocrystals.[2,3,5,6,25] Magnetic circularly polarized luminescence (MCPL) spectroscopy has been used to study Zeeman splittings in MBE-grown QDs[16,21–23,26] but has not previously been applied to any colloidal semiconductor nanocrystals. Parts a−c of Figure 4 show low-temperature absorption, MCD, and MCPL spectra of large colloidal Mn^{2+}:CdSe nanocrystals ($d \approx 4.2$ nm, 4.5% Mn^{2+}:CdSe), respectively. The magnetic field dependence of the MCD and MCPL intensities are summarized in parts d and e of Figures 4, respectively. For comparison, the MCD and MCPL intensities of undoped CdSe nanocrystals of similar size are also plotted in parts d and e of Figure 4, respectively. Both magneto-optical techniques show intense field-dependent features at the first exciton of the Mn^{2+}:CdSe nanocrystals

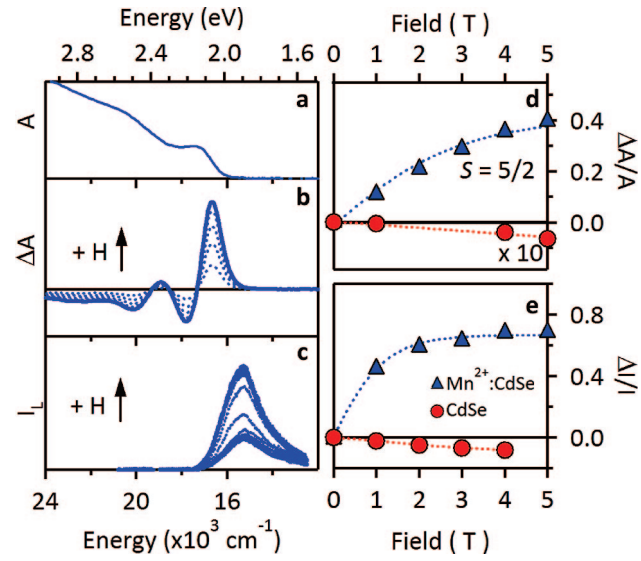

Figure 4. Magneto-optical spectroscopic results for colloidal Mn^{2+}:CdSe and CdSe quantum dots. (a) 6 K absorption, (b) 6 K MCD (0–5 T), and (c) 2 K (nominal) MCPL (I_L, –5 to +5 T) spectra of $d \approx 4.2$ nm 4.5% Mn^{2+}:CdSe quantum dots. (d) MCD, and (e) MCPL polarization ratios $[(I_L - I_R)/(I_L + I_R)]$ for both $d \approx 4.2$ nm 4.5% Mn^{2+}:CdSe (▲) and $d \approx 4.0$ nm CdSe (●) quantum dots as a function of magnetic field. For discussion of sign convention, see Supporting Information.

but much weaker field dependence for the analogous undoped nanocrystals. The undoped CdSe MCD intensities increase linearly with applied magnetic field, while those of the doped CdSe nanocrystals saturate following $S = 5/2$ Brillouin magnetization. Finally, the MCD and MCPL signal intensities are both inverted in the Mn^{2+}:CdSe nanocrystals relative to the undoped CdSe nanocrystals (Figure 4d,e), which indicates

that the signs of the QD excitonic Zeeman splittings (i.e., the effective g-factors) are reversed upon doping.

For these nanocrystals, the signs of the excitonic Zeeman splittings are determined by the competition between intrinsic (int) and exchange-induced (sp-d) splitting energies in the nanocrystals as described by eq 1:[6,16,22,27]

$$\Delta E_{\text{Zeeman}} = g_{\text{eff}}(\text{int})\mu_B H + x_{\text{eff}}\langle S_z\rangle N_0(\alpha - \beta) \qquad (1)$$

where α and β represent electron− and hole−Mn^{2+} magnetic exchange integrals, $\langle S_z\rangle$ is the temperature- and field-dependent Mn^{2+} spin expectation value in the direction of the applied magnetic field, x_{eff} is the effective Mn^{2+} mole fraction, and N_0 is the cation density.[24] In undoped QDs ($x_{\text{eff}} = 0$), the excitonic Zeeman splitting is determined solely by the intrinsic electron and hole Landé g factors, shown theoretically to be $g_{\text{eff}}(\text{int}) = (3g_h - g_e) \approx +1.5$ for similar CdSe nanocrystals.[25] Previous MCD experiments on similar undoped colloidal CdSe nanocrystals have measured $g_{\text{eff}}(\text{int}) \approx +1.0$ to $+1.5$.[6,25] For $x_{\text{eff}} > 0$, the second term in eq 1 contributes in proportion to x_{eff}, $\langle S_z\rangle$, and N_0 $(\alpha - \beta)$. In both bulk and nanocrystalline Mn^{2+}:CdSe, N_0 $(\alpha - \beta) \approx +1.5$ eV[16,24] and $-5/2 < \langle S_z\rangle < 0$,[24] resulting in a negative sp-d contribution to ΔE_{Zeeman} with $S = 5/2$ saturation magnetization. The $S = 5/2$ excitonic MCD saturation magnetization observed in Figure 4d, along with the inverted signs of the band-edge MCD and MCPL intensities (Figure 4d,e), thus directly indicate that carrier−Mn^{2+} sp-d exchange dominates the excitonic Zeeman splittings of these colloidal Mn^{2+}-doped CdSe nanocrystals. Quantitative analysis of the MCD intensities in Figure 4 via methods outlined previously[2,3,5,6,25] (see Supporting Information) yields $\Delta E_{\text{Zeeman}} \approx -55$ meV at saturation, and $g_{\text{eff}} \approx -300$ at $H = 0.1$ T, 6 K.

Quantitative analysis of the MCPL intensities in Figure 4e is more complex, and two salient features warrant discussion. First, $\Delta I/I$ requires a greater magnetic field to reach saturation than would be expected based on the Zeeman splittings determined from MCD spectroscopy. Very similar behavior was observed for the MBE-grown 7% Mn^{2+}:CdSe QDs of ref 21. This curvature is highly sensitive to sample temperature, however, and the data can be reproduced using the MCD Zeeman parameters by assuming $T = 35$ K instead of the cryostat temperature of 2 K (see Supporting Information). This result therefore suggests a modest increase in the Mn^{2+} spin temperature by laser heating during the MCPL measurement and could arise from slow Mn^{2+} spin–lattice relaxation or from a nonequilibrium lattice temperature, both of which have been described previously for MBE-grown DMS quantum wells.[28,29] Such laser heating effects may be exacerbated in these colloids by their isolation in the frozen glassy matrix.

Second, the MCPL dichroism ratio $\Delta I/I$ saturates at a value of 0.7 rather than at 1.0. This reduced value cannot be related to the magnetic fluctuations, laser heating, or slow polaron orientation effects discussed previously[28–31] because $\Delta I/I$ is independent of magnetic field under saturation conditions (Figure 4e), whereas each of these effects should be magnetic-field dependent. Contribution from nonpolarized trap emission can also be ruled out because the LCP spectrum retains its band shape at all fields (see Figure 4c), even at high negative fields where LCP emission should not be observed if emission occurred only from the lowest Zeeman component of the exciton. MCPL saturation values below 1.0 have also been reported for analogous MBE-grown Mn^{2+}:CdSe QDs,[21,22] and slow excitonic spin–lattice relaxation was proposed as one possible explanation for that reduced $\Delta I/I$ at saturation.[22] In contrast with MCD intensities, MCPL intensities can be influenced by thermalization dynamics,[32] and complete Boltzmann thermalization requires the emitting state's lifetime (τ_{exc}) to be long relative to its spin–lattice relaxation time (τ_S). Application of the analysis used for the MBE-grown Mn^{2+}:CdSe QDs of ref 22 to the data in Figure 4e would yield a ratio of $\tau_{\text{exc}}/\tau_S \approx 2.3$, which would imply unexpectedly slow excitonic spin–lattice relaxation in these colloidal Mn^{2+}:CdSe nanocrystals. This comparison suggests that experiments focused on measuring excitonic spin–lattice relaxation times in these colloidal DMS nanocrystals may provide important new insight into spin dynamics in free-standing DMS nanostructures. The development of colloidal DMS nanocrystals described by scenario III in Figure 1 reported here makes such experiments now possible. Despite this reduced saturation ratio, the value of $\Delta I/I = 0.7$ shown in Figure 4e clearly demonstrates the existence of excitonic spin polarization due to exchange interactions with the Mn^{2+} dopants. The MCPL polarization ratio in Figure 4e is larger than that reported for MBE-grown 2% Mn^{2+}:CdSe QDs ($\Delta I/I \approx 0.1$),[22] and overall the data in Figure 4 are very similar to those reported for MBE-grown 7% Mn^{2+}:CdSe QDs, which show $\Delta I/I \approx 1.0$ and $g_{\text{eff}} \approx 300$ in ref 16, and $\Delta I/I \approx 0.8$ in ref 21. The unique aspect of the data in Figure 4 is that these data were collected on *colloidal* Mn^{2+}:CdSe quantum dots.

The nanocrystals of Figure 4 differ from all other colloidal DMS nanocrystals reported to date in that they are the first to show excitonic emission that is not quenched by energy transfer to the dopants. Two magneto-optical techniques independently confirm the existence of giant excitonic Zeeman splittings in these colloids comparable to those of the best MBE-grown DMS QDs. When compared with MBE samples, however, these colloidal DMS nanocrystals have the added feature that they are processable, allowing purification, handling, and ultimately integration into spin-electronic or spin-photonic device architectures using soft chemistry techniques, and they therefore introduce new opportunities for studying and applying DMSs in nanotechnology.

Acknowledgment. Financial support from the NSF (PECASE DMR-0239325 to D.G. and DMR-0603752 to M.D. and J.F.), the Research Corporation (Cottrell Scholar to D.G.), the Dreyfus Foundation (Teacher/Scholar to D.G.), the NSERC postdoctoral fellowship program (to R.B.), and the Seoul R&DB Program (to S.L.) is gratefully acknowledged. We thank Jos van Rijssel and Prof. Andries Meijerink at Utrecht University for assistance with the photoluminescence lifetime measurements.

Supporting Information Available: Additional experimental information, a discussion of sign conventions, compilation of other colloidal DMS nanocrystal data, MCPL data for undoped nanocrystals, and simulated saturation magne-

tization curves. This material is available free of charge via the Internet at http://pubs.acs.org.

References

(1) Bryan, J. D.; Gamelin, D. R. *Prog. Inorg. Chem.* **2005**, *54*, 47–126.
(2) Hoffman, D. M.; Meyer, B. K.; Ekimov, A. I.; Merkulov, I. A.; Efros, A. L.; Rosen, M.; Counio, G.; Gacoin, T.; Boilot, J.-P. *Solid State Commun.* **2000**, *114*, 547–550.
(3) Norris, D. J.; Yao, N.; Charnock, F. T.; Kennedy, T. A. *Nano Lett.* **2001**, *1*, 3–7.
(4) Schwartz, D. A.; Norberg, N. S.; Nguyen, Q. P.; Parker, J. M.; Gamelin, D. R. *J. Am. Chem. Soc.* **2003**, *125*, 13205–13218.
(5) Norberg, N. S.; Parks, G. L.; Salley, G. M.; Gamelin, D. R. *J. Am. Chem. Soc.* **2006**, *128*, 13195–13203.
(6) Archer, P. I.; Santangelo, S. A.; Gamelin, D. R. *Nano Lett.* **2007**, *7*, 1037–1043.
(7) Norberg, N. S.; Kittilstved, K. R.; Amonette, J. E.; Kukkadapu, R. K.; Schwartz, D. A.; Gamelin, D. R. *J. Am. Chem. Soc.* **2004**, *126*, 9387–9398.
(8) Suyver, J. F.; Wuister, S. F.; Kelly, J. J.; Meijerink, A. *Phys. Chem. Chem. Phys.* **2000**, *2*, 5445–5448.
(9) Suyver, J. F.; van der Beek, T.; Wuister, S. F.; Kelly, J. J.; Meijerink, A. *Appl. Phys. Lett.* **2001**, *79*, 4222–4224.
(10) Bol, A. A.; Meijerink, A. *Phys. Rev. B* **1998**, *58*, 15997–16000.
(11) Wang, S.; Jarrett, B. R.; Kauzlarich, S. M.; Louie, A. Y. *J. Am. Chem. Soc.* **2007**, *129*, 3848–3856.
(12) Pradhan, N.; Battaglia, D. M.; Liu, Y.; Peng, X. *Nano Lett.* **2007**, *7*, 312–317.
(13) Erwin, S. C.; Zu, L. J.; Haftel, M. I.; Efros, A. L.; Kennedy, T. A.; Norris, D. J. *Nature* **2005**, *436*, 91–94.
(14) Norberg, N. S.; Dalpian, G. M.; Chelikowsky, J. R.; Gamelin, D. R. *Nano Lett.* **2006**, *6*, 2887–2892.
(15) Archer, P. I.; Santangelo, S. A.; Gamelin, D. R. *J. Am. Chem. Soc.* **2007**, *129*, 9808–9818.
(16) Hundt, A.; Puls, J.; Henneberger, F. *Phys. Rev. B* **2004**, *69*, 121309(R).
(17) Mikulec, F. V.; Kuno, M.; Bennati, M.; Hall, D. A.; Griffin, R. G.; Bawendi, M. G. *J. Am. Chem. Soc.* **2000**, *122*, 2532–2540.
(18) Magana, D.; Perera, S. C.; Harter, A. G.; Dalal, N. S.; Strouse, G. F. *J. Am. Chem. Soc.* **2006**, *128*, 2931–2939.
(19) Jian, W. B.; Fang, J.; Ji, T.; He, J. *Appl. Phys. Lett.* **2003**, *83*, 3377–3379.
(20) Guo, B. C.; Pang, Q.; Yang, C. L.; Ge, W. K.; Yang, S. H.; Wang, J. N. *AIP Conf. Proc.* **2005**, *772*, 605–606.
(21) Chernenko, A. V.; Dorozhkin, P. S.; Kulakovskii, V. D.; Brichkin, A. S.; Ivanov, S. V.; Toropov, A. A. *Phys. Rev. B* **2005**, *72*, 045302.
(22) Schmidt, T.; Scheibner, M.; Worschech, L.; Forchel, A.; Slobodskyy, T.; Molenkamp, L. W. *J. Appl. Phys.* **2006**, *100*, 123109.
(23) Lee, S.; Shin, D. Y.; Titova, L. V.; Kutrowski, M.; Furdyna, J. K.; Dobrowolska, M. *J. Supercond.* **2003**, *16*, 453–456.
(24) Furdyna, J. K.; Kossut, J. *Diluted Magnetic Semiconductors;* Vol. 25 in Semiconductors and Semimetals; Willardson, R. K., Beer, A. C., Eds.; Academic Press: New York, 1988.
(25) Kuno, M.; Nirmal, M.; Bawendi, M. G.; Efros, A.; Rosen, M. *J. Chem. Phys.* **1998**, *108*, 4242–4247.
(26) Lee, S.; Dobrowolska, M.; Furdyna, J. K. *Solid State Commun.* **2007**, *141*, 311–315.
(27) Bacher, G. *Top. Appl. Phys.* **2003**, *90*, 147–185.
(28) Kneip, M. K.; Yakovlev, D. R.; Bayer, M.; Maksimov, A. A.; Tartakovskii, I. I.; Keller, D.; Ossau, W.; Molenkamp, L. W.; Waag, A. *Phys. Rev. B* **2006**, *73*, 045305.
(29) Koudinov, A. V.; Kusrayev, Y. G.; Aksyanov, I. G. *Phys. Rev. B* **2003**, *68*, 085315.
(30) Merkulov, I. A.; Yakovlev, D. R.; Kavokin, K. V.; Mackh, G.; Ossau, W.; Waag, A.; Landwehr, G. *JETP Lett.* **1995**, *62*, 335–339.
(31) Bacher, G.; Maksimov, A. A.; Schömig, H.; Kulakovskii, V. D.; Welsch, M. K.; Forchel, A.; Dorozhkin, P. S.; Chernenko, A. V.; Lee, S.; Dobrowolska, M.; Furdyna, J. K. *Phys. Rev. Lett.* **2002**, *89*, 127201.
(32) Piepho, S. B.; Schatz, P. N., *Group Theory in Spectroscopy with Applications to Magnetic Circular Dichroism*; Wiley: New York, 1983.

NL080195P